

**In the honour  
of  
My loving family**



## **Certificate**

It is certified that the work contained in the thesis titled "**Collective behavior of polar self propelled particles with inhomogeneity**" by **Mr. Jay Prakash Singh**, Roll Number **16171008**, has been carried out under my/our supervision and that this work has not been submitted elsewhere for a degree.

**Signature:**

**Supervisor  
(Affiliation)**

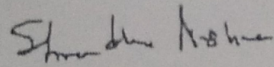
**Co-Supervisor  
(Affiliation)**

**External Supervisor  
(Affiliation)**

## Certificate

It is certified that the work contained in the thesis titled "Collective behavior of polar self propelled particles with inhomogeneity" by Mr. Jay Prakash Singh, Roll Number 16171008, has been carried out under my/our supervision and that this work has not been submitted elsewhere for a degree.

Signature:



Supervisor

(Affiliation)

*Assistant Professor*

Department of Physics

Indian Institute of Technology

(Banaras Hindu University)

Varanasi-221005

Co-Supervisor

(Affiliation)

External Supervisor

(Affiliation)

## Declaration

I, **Jay Prakash Singh**, certify that the work embodied in this thesis is my own bonafide work and carried out by me under the supervision of **Dr. Shradha Mishra** from July 2016 to July, 2021 at the **Department of Physics**, Indian Institute of Technology (BHU), Varanasi. The matter embodied in this thesis has not been submitted for the award of any other degree/diploma. I declare that I have faithfully acknowledged and given credits to the research workers whenever and wherever their works have been cited in my work in this thesis. I further declare that I have not wilfully copied any others' work, paragraphs, text, data, results, etc., reported in journals, books, magazines, reports dissertations, theses, etc., or available at websites and have not included them in this thesis and have not cited as my own work.

Date

Signature

Place

**Jay Prakash Singh**

## Certificate by the Supervisor

It is certified that the above statement made by the student is correct to the best of my knowledge.

**Signature:**

**Supervisor  
(Affiliation)**

**Co-Supervisor  
(Affiliation)**

**External Supervisor  
(Affiliation)**

Signature of the Head of the Department

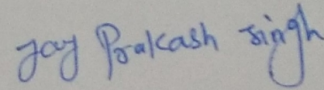
(Department)

## Declaration

I, **Jay Prakash Singh**, certify that the work embodied in this thesis is my own bonafide work and carried out by me under the supervision of **Dr. Shradha Mishra** from July 2016 to July, 2021 at the **Department of Physics**, Indian Institute of Technology (BHU), Varanasi. The matter embodied in this thesis has not been submitted for the award of any other degree/diploma. I declare that I have faithfully acknowledged and given credits to the research workers whenever and wherever their works have been cited in my work in this thesis. I further declare that I have not wilfully copied any others' work, paragraphs, text, data, results, etc., reported in journals, books, magazines, reports dissertations, theses, etc., or available at websites and have not included them in this thesis and have not cited as my own work.

Date

Signature



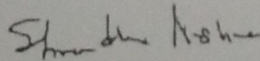
Place

Jay Prakash Singh

## Certificate by the Supervisor

It is certified that the above statement made by the student is correct to the best of my knowledge.

Signature:



Supervisor

Co-Supervisor

External Supervisor

(Affiliation)

(Affiliation)

(Affiliation)

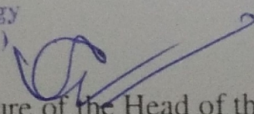
Assistant Professor

Department of Physics

Indian Institute of Technology

(Banaras Hindu University)

Varanasi-221005


  
Signature of the Head of the Department

(Department)

HEAD/ विभागाध्यक्ष

भौतिकी विभाग/Deptt. of Physics

भा०प्रौ०सं०/(का०हि०वि०)/IIT (BHU)

वाराणसी/Varanasi-221005

# Copyright Transfer Certificate

Title of the Thesis: "**Collective behavior of polar self propelled particles with inhomogeneity**"

Name of the Student : Jay Prakash Singh

## Copyright Transfer

The undersigned hereby assigns to the Institute of Technology (Banaras Hindu University) Varanasi all rights under copyright that may exist in and for the above thesis submitted for the award of the **Doctor of Philosophy (Ph.D) in Physics**.

Date

Signature

Place

Jay Prakash Singh

**Note: However, the author may reproduce or authorize others to reproduce material extracted verbatim from the thesis or derivative of the thesis for author's personal use provided that the source and the Institute's copyright notice are indicated.**

## Copyright Transfer Certificate

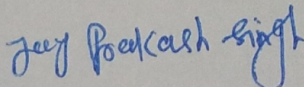
Title of the Thesis: "Collective behavior of polar self propelled particles with inhomogeneity"

Name of the Student : Jay Prakash Singh

### Copyright Transfer

The undersigned hereby assigns to the Institute of Technology (Banaras Hindu University) Varanasi all rights under copyright that may exist in and for the above thesis submitted for the award of the **Doctor of Philosophy (Ph.D)** in **Physics**.

Date

Signature 

Place

Jay Prakash Singh

**Note:** However, the author may reproduce or authorize others to reproduce material extracted verbatim from the thesis or derivative of the thesis for author's personal use provided that the source and the Institute's copyright notice are indicated.

## Acknowledgements

I would like to express my spacial gratitude to all those people for their constant support, love, affection, I got throughout this journey. Here, I have made mere attempt to name a few.

First of all, I would like to express my sincere thanks to my respected supervisor, ***Dr. Shradha Mishra, Department of Physics, IIT(BHU), Varanasi***, for her excellent guidance, continuous encouragement, patience, advice and moral support during the whole span of Ph.D. I feel very lucky to have such a supervisor who cared so much about my work, has shaped my understanding on the subject and has given me confidence to work independently. I also learnt from her which is much more than one could have expected from the supervisor.

I express my cordial thanks to ***Dr. Manoranjan Kumar and Dr. Jaydeb Chakrabarti, S.N.Bose National Centre for Basic Science Kolkata, Dr. D. P Giri, Department of Physics IIT(BHU), and RPEC member Dr. Preetam Singh, Department of ceramic engineering IIT(BHU)*** for their continuous encouragement and support throughout my research work. I wish to thank my fellow lab mates (*Sameer Kumar, Vivek Semwal, Shambhavi Dikshit, Pawan Mishra and Pratikshya*) of the Soft-matter group in the Department for their help and support.

Further, I would like to extend my thanks to my seniors ***Dr. Rakesh Das, and Dr. Sudipta Pattanayak***, for helping me a lot like brother. I am also grateful to my Institute, IIT(BHU), for providing necessary resources institute computing facility and super computing facility ***PARAM SHIVAY*** throughout my research. I express my thanks to all teaching and non teaching staff members of the department for their supports. I gratefully acknowledge Institute fellowship IIT(BHU), for providing the fellowship in form of Junior Research Fellowship and Senior Research fellowship.

I express my sincere and cordial gratitude to my father *Shri. Triyugi Narayan Singh*, my mother *Smt. Geeta Devi*, my younger brother *Mr. Om Prakash Singh*, my younger sister *Gudia* and my friend *Miss. Honey Tiwari* who always stood by my decisions and provided all kinds of supports, moral as well as financial. It was their love, care and patience which encouraged me to move on. The person with the greatest indirect contribution to this work is my grandfather, *Late. Shri Ram Shiromani Singh*, for his deepest love, endless patience and continued support shown in course of my research work.

This acknowledgement would be incomplete if the name of great visionary *Pt. Madan Mohan Malaviya* is not mentioned, who made this divine centre of knowledge. Deepest regards to him. Above all, praises and thanks to the God, the Almighty, for his showers of blessings throughout my research work, who has made everything possible.

**Department of Physics, IIT (BHU)**

**Jay Prakash Singh**

# Abstract

The study of active systems is an active area of current research in soft matter physics. Active systems show fascinating collective behavior and statistical properties which include both living and non-living matter. These systems are composed of self-driven units, self-propelled particles, and each has the ability to transduce stored energy into systematic movement, for example: a swarm of myxobacteria, cytoskeleton of living cells, bacterial suspensions, cell layers, terrestrial and aquatic animals, aerial flocks, and colloidal systems. A distinct feature of active matter systems compared to other nonequilibrium systems is that the energy input at the level of each particle drives the system out of equilibrium.

In this thesis, we discuss various properties of a collection of polar particles and also the dynamics of a single polar particle. Further, we study the effects of intrinsic inhomogeneities in polar systems and also the growth kinetics of the polar systems. Moreover, we also use the mean-field theory and linearization approximation to solve hydrodynamic equations of motion written from the symmetry arguments and the associated conservation laws. This thesis is organized into seven chapters.

Chapter 1 is the introduction which describes active systems and the historical background of the problem. This chapter includes definition and basic properties of active systems. We also discuss the different approaches to study the active systems like: agent-based simulation and hydrodynamic equations of motion. The rest of the chapters are organised as follows:

In chapter 2, we model a binary mixture of self-propelled particles moving with variable speed. The variable speed model is introduced, where the propulsion speed of each particle varies with their neighbour's orientation ( $\chi(t)$ ) through a power exponent  $\gamma$  such that  $v(t) = v_o |\chi(t)|^\gamma$ . Where  $v(t)$  is the self-propulsion speed of the particles at time  $t$  and  $v_o$  is the maximum self-propulsion speed. Two types of particles can be characterised by

different power exponents  $\gamma_1$  and  $\gamma_2$ . In the ordered state, we find phase separation when the difference in the two's exponent is large. In the disordered state, when the difference in the two's exponents is large, one type of particle with a large exponent forms static clusters, which act as a nucleation site for another type of particle with smaller exponents.

In chapter3, we introduce a minimal model for a collection of polar self-propelled particles with the bond disorder in the deep-ordered state. We find that the presence of the disorder does not destroy the usual long-range ordering in the system. Further, density clustering is enhanced, hence there is more cohesion in the presence of the disorder. Furthermore, ordering kinetics and giant number fluctuation does not change with bond disorder.

Chapter4 describes the study of the polar flock with bond disorder near the order-disorder transition. We find that the nature of the phase transition changes from discontinuous to continuous by tuning the strength of the disorder. The bond disorder also enhances the ordering near the transition due to the formation of a homogeneous -flock state for the large disorder. It leads to faster information transfer in the system and enhances the systems' information entropy.

In chapter5, we study the properties of polar self-propelled particles along a thin junction. Inside the junction, particles experience a high noise-disorder state, and outside they are in the ordered state. The width of the junction is adjusted by the junction width parameter 'd'. The model is motivated by the Josephson junction, an analogous equilibrium system. At the junction, we have found the current orientation reversal for a critical width of the junction, which is a common feature of the Josephson junction. Further, the particle current at the junction decreases with an increase in the junction width.

In chapter6, we studied the phases of passive disk-shaped particles of different sizes with external potential on a two dimensional substrate using overdamped Langevin dynamics. Where the potential is obtained from the binary mixture of active and passive particles for variable size ratio S and activity. We find potential is an attractive type for small distances

for large size ratio and activity. Four different phases are found: (1) homogeneous disorder phase (HDP), (2) homogeneous crystal phase (HCP), (3) disordered phase separated phase (DPS), and finally, (4) ordered phase-separated phase (OPS). Moreover, the system is studied in two ways viz: microscopic and coarse-grain simulation. The observed phases are consistent in both ways.

Finally, in Chapter 7, we conclude the thesis with a brief summary of all the chapters discussed above with future prospects.



# Table of contents

<b>List of figures</b>	<b>xxi</b>
<b>1 Introduction</b>	<b>1</b>
1.1 Statistical mechanics and its evolution . . . . .	1
1.2 Active matter system . . . . .	5
1.2.1 Types of active matter system . . . . .	7
1.2.2 Types of active particles . . . . .	8
1.3 Role of disorder or inhomogeneity among SPPs . . . . .	11
1.4 Methodology . . . . .	12
1.4.1 Agent or microscopic rule based simulation . . . . .	13
1.4.2 Phenomenology : hydrodynamic equations of motion . . . . .	19
1.4.3 Homogeneous steady states . . . . .	22
1.4.4 Two-point correlations and giant number fluctuations . . . . .	23
1.4.5 Scaling and ordering kinetics . . . . .	23
1.5 Objective and organisation of this thesis . . . . .	24
1.6 Technical details . . . . .	27
<b>2 Phase separation in a binary mixture of self-propelled particles with variable speed</b>	<b>29</b>
2.1 Introduction . . . . .	29

2.2	Model . . . . .	32
2.3	Results . . . . .	34
2.3.1	Ordered Phase Separated: OPS . . . . .	37
2.3.2	Ordered Mixed: OM . . . . .	38
2.3.3	Disordered Mixed: DM . . . . .	39
2.3.4	Disordered Phase Segregated: DPS . . . . .	40
2.3.5	Dynamics of particle in DM and DPS phase . . . . .	41
2.4	Coarse-grained hydrodynamics . . . . .	42
2.5	Linearised study of hydrodynamic equations of motion . . . . .	45
2.6	Discussion . . . . .	49
<b>3</b>	<b>Ordering kinetics and steady state of self-propelled particles with random-</b>	
	<b>bond disorder</b>	<b>51</b>
3.1	Introduction . . . . .	51
3.2	Model . . . . .	53
3.3	Results . . . . .	56
3.3.1	Steady-state behaviour . . . . .	56
3.4	Dynamical Behaviour . . . . .	63
3.4.1	Ordering kinetics to the steady state . . . . .	63
3.5	Linearised study of hydrodynamic equations of motion . . . . .	64
3.6	Discussion . . . . .	69
<b>4</b>	<b>Bond disorder enhances the information transfer in the polar flock</b>	<b>71</b>
4.1	Introduction . . . . .	71
4.2	Model . . . . .	73
4.3	Results . . . . .	75
4.3.1	Disorder-to-order transition . . . . .	75

---

4.3.2	Properties of the polar flock . . . . .	80
4.3.3	Accelerated response to external perturbation . . . . .	81
4.3.4	Disorder increases the systems' information entropy . . . . .	83
4.4	Discussion . . . . .	86
<b>5</b>	<b>Collection of self-propelled particles across an order-disorder interface</b>	<b>89</b>
5.1	Introduction . . . . .	89
5.2	Model . . . . .	91
5.3	Results . . . . .	93
5.3.1	Steady state behaviour . . . . .	93
5.4	Summary and discussion . . . . .	98
<b>6</b>	<b>Phases of passive colloids in activity driven bath</b>	<b>101</b>
6.1	Introduction . . . . .	101
6.2	Model . . . . .	104
6.3	Results . . . . .	108
6.3.1	Calculation of depletion force . . . . .	108
6.3.2	Coarse-grained simulation of pure passive system . . . . .	109
6.3.3	Four distinct phases . . . . .	109
6.4	Phase diagram . . . . .	112
6.5	Discussion . . . . .	113
<b>7</b>	<b>Summary and conclusion</b>	<b>117</b>
7.1	Summary . . . . .	117
7.2	Future prospects . . . . .	118
	<b>References</b>	<b>121</b>
	<b>List of Publications</b>	<b>i</b>



# List of figures

- 1.1 Schematic of the various types of active particles and orientationally ordered states. Polar active particles (top left image), such as bacteria or birds, have a head and a tail and are generally self-propelled along their long axis. They can order in polar states (bottom left) or nematic states (bottom center). The polar state is also a moving state with a non-zero mean velocity. Apolar active particles (top center image) are head-tail symmetric and can order in nematic states (bottom right). Self-propelled rods (top right image) are head-tail symmetric, but each rod is self-propelled in a specific direction along its long axis. The self-propulsion renders the particles polar, but for exclusively apolar interactions (such as steric effects), self-propelled rods can order only in nematic states (bottom center). 9

- 1.2 In this figure the velocities of the particles are displayed for varying values of the density and the noise. The actual velocity of a particle is indicated by a small arrow. Four snapshots show the different phases of SPPs with respect to density and noise. (a) At time  $t = 0$ ,  $L = 50$ ,  $N = 1340$ ,  $\rho = 0.5$  and  $\eta = 0.7$ . (b) At time  $t = 500$ , For small densities and noise the particles tend to form groups moving coherently in random directions,  $L = 50$ ,  $N = 1340$ ,  $\rho = 0.5$  and  $\eta = 0.2$ (c) After some time at higher densities and noise the particles move randomly with some correlation  $L = 100$ ,  $N = 2430$ ,  $\rho = 1.0$  and  $\eta = 0.7$ . (d) For higher density and small noise, the motion becomes ordered  $L = 100$ ,  $N = 2430$ ,  $\rho = 1.0$  and  $\eta = 0.2$ . All of our results shown in Figs.(a)-(d) were obtained from simulations in which velocity  $v = 0.5$ . . . . . 15
- 2.1 (color online) Top panel: real space snapshots of position of two types of particles with the direction of their velocity vectors. Color represents two types of particles. Black is for particle of type one and red for second type particle. (a) is for initial random homogeneous mixed state, (b) is for ordered phase separated state ( $\gamma_2 = 8$ ,  $\eta = 0.2$ ), (c) ordered mixed ( $\gamma_2 = 0.5$   $\eta = 0.2$ ), (d) is for disordered mixed ( $\gamma_2 = 0.5$ ,  $\eta = 0.62$ ) and (e) is for disordered phase segregated phase ( $\gamma_2 = 8$ ,  $\eta = 0.62$ ). (Bottom panel) (b'-e') are the zoomed version of top panel plot for better clarity of four different phases. All snapshots are collected in the steady state and plots are a part of the full system of size  $L = 100$  or  $N = 10^4$ . . . . . 31

- 2.2 (color online) Plot of orientation order parameter (OOP) vs. noise strength  $\eta$ ,  $\gamma_1 = 1$ , different curves are for different  $\gamma_2$ .  $\circ$ ,  $\square$ ,  $\diamond$  and  $\triangle$  are for  $\gamma_2 = 0.5, 2, 4$  and  $6$  respectively. Empty symbols denote data for  $L = 100$ , or  $N = 10^4$  and filled ones are for  $L = 200$  or  $N = 4 \times 10^4$ . For  $L = 200$  more number of data points are obtained near order-to-disorder phase transition. For all  $\gamma_2$ , critical noise lies between  $0.57 - 0.60$ . Total simulation time is  $10^7$  and data is extracted from last  $10^6$  times in the steady state. Averaging is done over five independent realisations. . . . . 35
- 2.3 (color online): Plot of DOP vs.  $\gamma_2$  for two different  $\eta = 0.2$  (*partially filled*) and  $0.62$  (*filled*). Other parameters are same as defined in Fig. 2.1. Different symbols denote the four different phases in the system (i) Green diamond represents OPS for ( $2 < \gamma_2$ ). (ii) Black circle shows OM phase ( $0 < \gamma_2 < 2$ ). (iii) Red square represents DM phase for  $0 < \gamma_2 < 2$  and (iv) Blue triangles for DPS phase for ( $2 < \gamma_2$ ). . . . . 36
- 2.4 Plot of PDF of speed  $P(v)$  vs.  $v$  for four different phases (a-d) for OPS, OM, DM and DPS respectively. The two curves are for  $P(v)$  for two types of particles.  $\circ$  and  $\square$  is for the particle of type one and two respectively. For all plots, there is always a peak at maximum speed  $v = v_0 = 0.5$  and second peak is at smaller  $v$  value. The difference in two peak positions is large for large  $\gamma_2$  in the ordered state. The shaded area ((b) and (c)) show the extent of mixing of particles of type one and two. Other parameters are same as in Fig.2.2 and  $N = 10^4$  . . . . . 38

- 2.5 (color online): Plot of particle number PDF,  $P_{ij}(n)$  for four different phases OPS, OM, DM and DPS, (a-d) respectively. Top panel is plot on normal scale and bottom is on log-log scale. The four curves in each panel are for four distributions as defined in the main text.  $\circ$ ,  $\square$ ,  $\diamond$  and  $\triangle$ 's are for  $P_{12}(n)$ ,  $P_{11}(n)$ ,  $P_{22}(n)$  and  $P_{21}(n)$  respectively. In the bottom panel curves are fitted with power-law and exponential tail for large  $n$ . Other parameters are same as in Fig. 2.1 . . . . . 39
- 2.6 Plot of normalised velocity difference  $\Delta V/v_0$  vs.  $\gamma_2$  for the ordered state  $\eta = 0.2$ . Other parameters are same as in Fig. 2.1 . . . . . 40
- 2.7 Plot of effective diffusivity  $D_{eff}$  vs.  $\gamma_2$  in the disordered region  $\eta = 0.65$  for two types of particles.  $\circ$ ,  $\square$  is for particle of type one and two respectively. Other parameters are same as given in Fig. 2.1 . . . . . 42
- 3.1 (color online) (a) Cartoon picture of the model. The dashed circle of radius  $R_I$  represents the interaction radius of the green tagged particle of radius  $R$  (at the centre). The circles of various colors of radius  $R$  indicate the neighbors of the tagged particle. The arrows of different lengths represent the interaction strength  $J$ 's of the respective particle. (b,c) The cartoon picture of the resultant direction of the tagged particle due to the alignment interaction with its neighbors for the uniform strength (clean polar flock) and the varying (RBDPF) interaction strength model, respectively. Black and green arrow represent the resultant directions of the tagged particle in (b) and (c), respectively. (d) The relative difference in the resultant direction  $\Delta\Omega_i$  of the tagged particle for the clean and the RBDPF. . . . . 55

- 3.2 (color online) (a) Plot of the global orientation order parameter  $\chi$  vs.  $1/N$  for different  $\varepsilon$  in semi-log X scale. (b) Probability distribution function of the mean orientation fluctuation  $P(\Delta\theta)$  vs.  $\frac{\Delta\theta}{\pi}$  for different  $\varepsilon$  in semi-log Y scale.  $N = 62500$ . The filled black circles, red squares, green diamonds represent data for  $\varepsilon = 0.0, 1.0,$  and  $2.0,$  respectively. (c,d) Plots of  $P(\Delta\theta)$  vs.  $\frac{\Delta\theta}{\pi}$  for different system sizes for  $\varepsilon = 0.0$  and  $\varepsilon = 2.0$  in semi-log Y scale, respectively. The filled black circles and red squares denote  $N = 40000$  and  $62500,$  respectively. . . . . 57

- 3.3 (color online) Horizontal panel: top to bottom panels are real space snapshots of the local number density of the SPPs for different  $\varepsilon$  at different times  $t$ . The topmost panel is for  $\varepsilon = 0,$  middle one is for  $\varepsilon = 1$  and bottom is for  $\varepsilon = 2.$  Vertical panels: from left to right, (a) to (c), are real snapshots of the local number density of the SPPs at different time  $t$  for each  $\varepsilon.$  Leftmost panel (a) is for  $t = 5,000,$  the middle one (b) is for  $t = 45,000$  and (c) represent zoomed snapshots of (b) at time  $t=45000.$  The square boxes in (c) represent the zoomed version of the square boxes of (b).  $N = 10,000.$  The color bar represents the local number density of the particles. . . . . 58

- 3.4 (color online) (a,b) Plots of  $P(n, \varepsilon)$  vs.  $n$  and  $P(n, \varepsilon)/P_o(\varepsilon)$  vs.  $n/n_c$  in semi-log Y scale for different  $\varepsilon$ , respectively. The black, red, orange, blue and green lines represent  $\varepsilon = 0.0, 0.5, 1.0, 1.5$ , and  $2.0$ , respectively. Inset of (a) is zoomed near to the peak of the distribution of main plot.  $N = 62500$ . In the *inset* of (b) Plot of  $\Delta n_c(\varepsilon) = n_c(\varepsilon) - n_c(0)$  vs.  $\varepsilon$ . Voilet circles represent the data obtained from the fitting function  $\exp(-n/n_c(\varepsilon))$  and orange dashed line indicates the linear variation. (c) Variation of local density fluctuation  $\Delta\Phi(\varepsilon)$  with  $\varepsilon$ . The filled black circles, blue squares and red triangles represent the numerical data points for  $\rho_0 = 0.5, 1$  and  $2$ , respectively. Error bars are in the order of symbol sizes.  $N = 62500$ . The black ( $\rho_0 = 0.5$ ), red ( $\rho_0 = 1.0$ ) and blue ( $\rho_0 = 2.0$ ) dashed line indicate the variation of  $\Delta\Phi(\varepsilon)$  obtained from the analytical calculations, as shown in Appendix.3.5 in Eq  $\sim((3.23))$ . (d) Plot of the global number fluctuation ( $\Delta\mathcal{N}$ ) vs. the mean number of particles  $\langle\mathcal{N}\rangle$  in log – log scale.  $N = 62500$ . The dashed line represents slope = 1.6. . . . . 61
- 3.5 (color online) (a) Snapshot of the neighbour particles within the interaction radius ( $R = 1.0$ ) of a tagged particle in the steady state for disorder strength  $\varepsilon = 2.0$ .  $N = 10000$ . The filled black circles, red squares, green diamonds, and blue triangles denote  $0 \leq J < 0.5$ ,  $0.5 \leq J < 1.0$ ,  $1.0 \leq J < 1.5$ , and  $1.5 \leq J \leq 2.0$ , respectively. At the centre of the box, yellow triangle indicates the tagged particle. (b,c) Plots of  $P(n_{J(i)})$  and  $P(\Delta\theta_{J(i)})$  distribution for different  $J(i)$  ranges, respectively.  $N = 62500$ . Color lines and symbols in (b,c) indicate same things as in (a). (d) Plot of normalise effective transport speed  $v(\varepsilon, t)/v_0$  vs.  $t$ . Black, red, green and blue lines represent  $\varepsilon = 0.0, 1.0, 1.5$  and  $2$  respectively.  $N = 10000$ . . . . . 62

- 3.6 (color online) (a,b) Plots  $C(r,t)$  vs.  $r/L_o$  for  $\varepsilon = 0$  and 2, respectively in semi-log Y-scale. Black, red, green, blue, cyan, brown and Violet lines represents time  $t = 2, 4, 16, 32, 64, 128$  and 256, respectively. In the *inset* of (a) and (b), the variation  $C(r,t)$  with  $r$  is shown at different time. Different colored lines represent same thing as the main figure. Dashed line with color magenta is drawn parallel to x-axis and intersect y-axis at 0.17 (crossing point) .  $N = 262144$  (c) Plot of  $L_o(t)$  with time  $t$  in log – log scale. The dashed line represents the slope 0.5.  $N = 262144$ . (d) Plot of mass of the largest cluster  $m(t)$  with time  $t$  in log – log scale.  $N = 40000$ . The dashed line represents the slope 0.5. The filled black circles, red squares, and green diamonds represent  $\varepsilon = 0.0, 1.0$  and 2.0, respectively. . 64

- 4.1 (color online) (a) The plot of the mean orientation order parameter  $\psi$  vs. noise strength  $\eta$ , *inset*: zoomed plot shows enhanced ordering on increasing  $\varepsilon$ . (b) Variation of susceptibility  $\xi$  vs.  $\varepsilon$ . (c) The probability distribution function of order parameter  $P(\psi)$  vs.  $\psi$  at the transition point ( $\eta_c(\varepsilon) = 0.625, 0.640,$  and 0.654 for  $\varepsilon = 0, 1$  and 2, respectively). (d) Variation of fourth-order Binder cumulant  $V$  vs.  $\eta$ . Different symbols imply different values of disorder strength  $\varepsilon = 0(\circ), 1.0(\square), 2.0(\triangle)$  for the system size  $L=150$  and the density  $\rho_N = 1.0$ . . . . . 76

- 4.2 (color online) Plot (a)-(c) show orientation order parameter  $\psi$  vs.  $\eta$  and (d-f) represent Binder cumulant  $V$  vs.  $\eta$  for  $\varepsilon = 0, 1$  and  $2$ . In plots (a)-(f) the black  $\circ$ , red  $\square$ , green  $\triangle$  and blue  $\star$  are for system sizes  $L = 90, 120, 150$  and  $200$ , respectively. (g)-(i) are plots of orientation order parameter distribution  $P(\psi)$  keeping system size  $L = 120$  for three different  $\eta$  values. (g) for  $\varepsilon = 0$ ,  $\eta = 0.6245, 0.6260$  and  $0.6275$ , (h)  $\varepsilon = 1$ ,  $\eta = 0.6375, 0.6390$  and  $0.6420$ , and (i)  $\varepsilon = 2$  for  $\eta = 0.6490, 0.6520$  and  $0.6540$ , respectively. Symbols with color black ‘+’, red ‘ $\star$ ’ and blue ‘ $\triangle$ ’ show the increase in  $\eta$  values with their respective  $\varepsilon$  values. In all the cases system density is fixed  $\rho_N = 1.0$ . . . . . 77
- 4.3 (color online) (a) Time series of  $\psi(t)$  for disorder  $\varepsilon = 1.0$  (black line) and  $\varepsilon = 2.0$  (magenta line). The two types of quenched impurities with orientations  $\pm \frac{\pi}{2}$  are introduced at time  $t = 10,000$ . (b) PDF for the orientation distribution  $P(\theta)$  vs. mean orientation  $\theta$ , for  $\varepsilon = 1.0$  ( $\square$ ) and  $\varepsilon = 2.0$  ( $\triangle$ ). All the plots are for system size  $L = 100$ , noise strength  $\eta = 0.62$  and the density  $\rho_N = 1.0$ . . . . . 78
- 4.4 (color online) Plot (a), (b) and (c) are the real space snapshots for three  $\varepsilon = 0, 1$  and  $2$ , respectively. The color bar shows the number of particles in the subshells. All the parameters are the same as in Fig.4.3. . . . . 79

- 4.5 (color online) (a) Plot of density phase separation order parameter  $\delta\phi$  vs.  $\varepsilon$  with blue squares. The blue dotted line shows the linear decay of  $\delta\phi$ . (b)  $P(n)$  vs.  $n$  for  $\varepsilon = 0, 0.5, 1, 1.5$  and  $2$ . Different colors with lines black, red, green, blue and magenta are for  $\varepsilon = 0, 0.5, 1.0, 1.5$  and  $2.0$ . The inset of Fig.(b) shows the mean number of particles  $N_c$  vs.  $\varepsilon$  where the blue dotted line shows linear decay of  $N_c$ . (c) and (d) show the zoom plot of (b) near to the head and tail where the tail parts are fitted with exponential function with dotted lines. Symbols with black (circles), red (squares), green (diamonds), blue(triangles up) and magenta (triangles left) colors are for  $\varepsilon = 0, 0.5, 1.0, 1.5$  and  $2.0$  in (c) and (d). Also, (b), (c) and (d) are in semi-log y-axis. All the parameters are the same as in Fig.4.3. . . . . . 80
- 4.6 (color online) (a) Plot of OACF  $C_0(r,t)$  vs.  $t$  for  $\varepsilon = 0.0$  (circles),  $0.5$  (squares),  $1.0$  (diamonds),  $1.5$  (triangles up) and  $2.0$  (triangles left). Dashed lines are fit to exponential to the data (symbols). (b) Plot for  $C_0(r,t)$  vs. scaled time  $t/t_c$ ; and  $t_c$  vs.  $\varepsilon$  (inset) where the dashed lines are a linear fit to the data. All other parameters are the same as in Fig. 4.3 . . . 82
- 4.7 (color online) (a), (b) and (c) show the variation of  $X(t)$  vs.  $t$ . Black, blue and magenta colors are for  $\varepsilon = 0, 1$  and  $2$ , respectively. (d) Variation of neighbour fluctuation autocorrelation  $C_n(r,t)$  vs.  $t$ . Symbols with black (circles), red (squares), green (diamonds), blue (triangles up) and magenta (triangles left) colors are for  $\varepsilon = 0, 0.5, 1.0, 1.5$  and  $2.0$ , respectively. Dashed lines are fit to exponential. (e) The plot of  $t_n$  vs.  $\varepsilon$  shows linear decay with  $\varepsilon$ ; inset; the plot of correlation  $C_n(r,t)$  vs. scaled time  $t/t_n$ . (f) The plot of the systems' information entropy  $\Delta S(t)$  vs.  $t$ . (g) Time evolution of  $\psi(t)$  with time  $t$  where colors black, blue and magenta are for  $\varepsilon = 0, 1$  and  $2$ , respectively. All other parameters are the same as in Fig. 4.3 83

- 4.8 (color online) The plot shows the probability of newly visited particles  $p(\varepsilon, t)$  with respect to time  $t$  for three values of  $\varepsilon$ . Black  $\circ$ , red  $\square$ , and blue  $\triangle$  are for  $\varepsilon = 0, 1$  and  $2$ , respectively. Color dotted lines show the data fit with fitting function  $p(\varepsilon, t) = m(\varepsilon) \cdot t$  where  $m(\varepsilon)$  is the slope. In the inset, we show the  $m$  vs.  $\varepsilon$  which increases linearly. Other parameters are the same as in Fig.4.3 . . . . . 85
- 5.1 (color online) We show a cartoon picture of the model. Left and right most box show the particles (SPPs) with arrows are, in the deep ordered state. Middle section shows the particles in disordered state. Noise strength for middle region  $\eta = 0.7$  and for rest of the region  $\eta = 0.3$  . . . . . 91
- 5.2 (color online) All the plots (a)-(d) shown here for without perturbation. (a) We plot the global orientation order parameter  $\Psi$  vs. width of the disorder region  $d$ . (b) Plot shows the global order parameter distribution  $P(\Psi)$  for different width of the junction 'd'. Different colored break lines are for  $d=4$  (black),  $d=8$  (red),  $d=12$  (green) and  $d=18$  (green). Plot (c) and (d) show the space snapshots of the system for width  $d=2$  and  $18$  respectively. Pink line shows the boundry of the junction and blue lines with arrow show the mean orientation of the local flock.  $L \times W = 200 \times 5$  and  $\rho = 1.0$  . . . 94

- 5.3 (color online) All the plots (a)-(d) shown here for with perturbation. (a) We plot the global orientation order parameter  $\Psi$  vs. width of the disorder region  $d$  with perturbation. (b) Plot shows the global order parameter distribution  $P(\Psi)$  for different width of the junction 'd'. Different colored break lines are for  $d=4$  (black),  $d=8$  (red),  $d=12$  (green) and  $d=18$  (green). Plot (c) and (d) show the space snapshots of the system for width  $d=2$  and  $18$  respectively. Pink lines show the bounry of the junction and blue lines with arrow show the mean orientation of the local flock.  $L \times W = 200 \times 5$  and  $\rho = 1.0$  . . . . . 95
- 5.4 (color online) Plot (a)-( show the time variation of event current  $\Psi_{xd}$  along the long axis with increasing width  $d$ . (d) event current distribution  $P(\Psi_{xd})$ . (e) Shows the x-orientation current autocorrelation for three junction width 'd'. Black, red and green colors show the results for junction width  $d=4,8$  and  $12$  respectively.  $L \times W = 200 \times 5$  and  $\rho = 1.0$ . . . . . 96
- 5.5 (color online) Plot (a)-(c) show the time variation of orientation event current  $\Psi_{yd}$  along the long axis with increasing width  $d$ . (d) Orientation event current distribution  $P(\Psi_{yd})$ . Black, red and green colors show the junction width  $d=4,8$  and  $12$  respectively.  $L \times W = 200 \times 5$  and  $\rho = 1.0$ . . . . . 97
- 5.6 (color online) Plot (a) show the global orientation order parameter  $\Psi_d$  with junction width 'd', and (b) show the probability distribution  $P(\Psi_d)$  for junction width  $d=4$  (black),  $8$  (red) and  $12$  (green) respectively.  $L \times W = 200 \times 5$  and  $\rho = 1.0$ . . . . . 98

- 6.1 (color online) Plot shows the model picture of small and big ABPs and passive system of  $S = 10$  to calculate the effective potential  $V^{S,\bar{v}}(r)$  on passive particle separated by distance 'r', exerted by the active depletant. Red particles show the ABPs. Blue and red particles show passive particles and ABPs. The blue arrow line show the surface to surface distance 'r' between two passive particles. Number of ABPs and passive particles are  $N_1 = 1000$  and  $N_2 = 2$  . . . . . 105
- 6.2 (color online) Plot shows the potential  $V^{S,\bar{v}}$  on passive particles in the presence of active depletant for different parameters  $(S, \bar{v})$ . Black curve (5, 60), green curve(10, 40), blue curve (5, 160) and red curve (10, 160) respectively. In all cases number of passive particles  $N_2 = 2$  and active particles are  $N_1 = 1000$ . . . . . 106
- 6.3 (color online) Steady-state snapshots for four phases of the passive particles interacting through the potential obtained with different combinations of activity  $\bar{v}$  and size ratio  $S$ . (a) HDP, for  $S, \bar{v} = 5, 60$  and packing fraction  $\phi_p = 0.07$ . (b) HCP for  $S, \bar{v} = 10, 40$  for  $\phi_p = 0.2$ . (c) DPS , for  $S, \bar{v} = 5, 160$  for  $\phi_p = 0.07$ . (d) OPS for  $S, \bar{v} = 10, 160$  and packing fraction  $\phi_p = 0.2$ . In all cases total number of passive particles are  $N_2 = 400$  . . . 107

- 6.4 (color online) We plot cluster size distribution CSD,  $P(n)$  vs. mean number of particles cluster  $n$  for four distinct phases. For HDP: (a) show the CSD for fixed  $S=4$  for different activity  $\bar{v} = 60$  (black circles),  $\bar{v} = 80$  (red square),  $\bar{v} = 100$  (orange diamonds) and (b) is for fixed  $\bar{v} = 60$  for different size ratio  $S=2$  (black circle),  $S=3$  (red square) and  $S=4$  (orange diamond). For HCP:(c) show the CSD for fixed  $S=10$  for different activity  $\bar{v} = 20$  (black circles) and  $\bar{v} = 40$  (red square) and (c) is for fixed  $\bar{v} = 40$  for different size ratio  $S=8$  (black circle),  $S=9$  (red square) and  $S=10$  (orange diamond). For DPS:(e) show the CSD for fixed  $S=7$  for different activity  $\bar{v} = 120$  (black circles),  $\bar{v} = 140$  (red square),  $\bar{v} = 160$  (orange diamonds) and (f) is for fixed  $\bar{v} = 160$  for different size ratio  $S=5$  (black circle),  $S=6$  (red square) and  $S=8$  (orange diamond). Finally, for OPS:(g) show the CSD for fixed  $S=10$  for different activity  $\bar{v} = 120$  (black circles),  $\bar{v} = 140$  (red square),  $\bar{v} = 160$  (orange diamonds) and (h) is for fixed  $\bar{v} = 160$  for different size ratio  $S=8$  (black circle),  $S=9$  (red square) and  $S=10$  (orange diamond). Other details are same as in Fig.6.3. Blue and pink lines show the slope of 2.0 and 3.5 respectively. . . . . 115
- 6.5 (color online) In this plot (a),(b), and (c), we show the phase diagram in  $S$ - $\bar{v}$  plane for  $\psi_6$ , mean cluster size  $m$ , and mean normalise distance  $r$ . In all the plots number of passive particles are 400. . . . . 116
- 6.6 (color online) Plot (a)-(d) show the distinct four phases obtained from microscopic simulation of ABPs and passive mixture with packing fraction  $\phi_a = 0.5$  and  $\phi_p = 0.2$ . (a) represents the HDP for  $(S, \bar{v}) = (5, 60)$ . (b) shows the HCP for  $(S, \bar{v}) = (10, 40)$ . (c) represents DPS for  $(S, \bar{v}) = (7, 160)$ . (d) shows the OPS for  $(S, \bar{v}) = (10, 160)$ . Smaller black particles are ABPs, and bigger are passive one. . . . . 116